PHILOSOPHICAL TRANSACTIONS OF THE ROYAL SOCIETY A MATHEMATICAL, PHYSICAL & ENGINEERING SCIENCES

Control of spatiotemporal chaos in catalytic CO oxidation by laser-induced pacemakers

Michael Stich, Christian Punckt, Carsten Beta and Harm Hinrich Rotermund

Phil. Trans. R. Soc. A 2008 **366**, 419-426
doi: 10.1098/rsta.2007.2099

PHILOSOPHICAL TRANSACTIONS OF THE ROYAL SOCIETY A

Phil. Trans. R. Soc. A (2008) **366**, 419–426
doi:10.1098/rsta.2007.2099
Published online 2 August 2007

Control of spatiotemporal chaos in catalytic CO oxidation by laser-induced pacemakers

By Michael Stich[1,*], Christian Punckt[2], Carsten Beta[3] and Harm Hinrich Rotermund[2,4]

[1]*Centro de Astrobiología (CSIC-INTA), Instituto Nacional de Técnica Aeroespacial, Ctra de Ajalvir km. 4, 28850 Torrejón de Ardoz, Madrid, Spain*
[2]*Fritz-Haber-Institut der Max-Planck-Gesellschaft, Faradayweg 4-6, 14195 Berlin, Germany*
[3]*Max-Planck-Institut für Dynamik und Selbstorganisation, Am Fassberg 11, 37077 Göttingen, Germany*
[4]*Department of Physics and Atmospheric Science, Dalhousie University, Halifax, Nova Scotia, Canada B3H 3J5*

Control of spatiotemporal chaos is achieved in the catalytic oxidation of CO on Pt(110) by localized modification of the kinetic properties of the surface chemical reaction. In the experiment, a small temperature heterogeneity is created on the surface by a focused laser beam. This heterogeneity constitutes a pacemaker and starts to emit target waves. These waves slowly entrain the medium and suppress the spatiotemporal chaos that is present in the absence of control. We compare this experimental result with a numerical study of the Krischer–Eiswirth–Ertl model for CO oxidation on Pt(110). We confirm the experimental findings and identify regimes where complete and partial controls are possible.

Keywords: pattern formation; chaos control; reaction–diffusion systems

1. Introduction

Besides regular wave patterns such as spiral or target waves, chemical reaction–diffusion systems are known to show spatiotemporally chaotic dynamics, also called chemical turbulence. Understanding spatiotemporal chaos has been a challenge for many years. Inspired by the work of Ott *et al.* (1990), recent contributions in this field have more and more focused on questions of chaos control.

A prototypical example of an experimental reaction–diffusion system is the catalytic oxidation of CO on Pt(110). Different regimes of self-organization have been studied in this system (Jakubith *et al.* 1990). Control of pattern formation and spatiotemporal chaos was achieved by applying global delayed feedback (Kim *et al.* 2001; Bertram *et al.* 2003*a*; Beta *et al.* 2003) as well as length-scale-dependent coupling (Beta *et al.* 2004) and periodic forcing (Bertram *et al.* 2003*b*). Many features of the experimentally observed dynamics under global control can be explained in the general framework of the complex Ginzburg–Landau

* Author for correspondence (stichm@inta.es).

One contribution of 15 to a Theme Issue 'Experimental chaos I'.

equation (Battogtokh & Mikhailov 1996; Beta & Mikhailov 2004). Recently, a new technique was established to locally address the dynamics of this surface chemical reaction by means of a focused laser beam (Wolff *et al.* 2001). This approach opens up new perspectives for the application of local control schemes.

Control of spatiotemporal chaos can lead to different regular dynamical states. One of the generic wave patterns in reaction–diffusion systems is the target pattern, consisting of concentric waves that are periodically emitted by a localized wave source called a pacemaker. Although stable pacemakers may result from the interplay of nonlinear kinetics and diffusion (Stich *et al.* 2001), most target patterns observed in experiments are due to small impurities such as dust particles or surface defects. Such heterogeneous pacemakers have attracted much interest (Stich & Mikhailov 2002, 2006) due to their presence in real systems, although they do not provide access for active pattern control due to their random appearance and unknown microscopic properties. Artificial pacemakers, on the other hand, can be readily created through appropriate localized modifications of the medium. For example, using the abovementioned laser-based technique, localized heterogeneities can be artificially introduced and studied in the CO oxidation system (Stich *et al.* 2004; Wolff *et al.* 2004). In the present investigation, we apply this approach to control spatiotemporal chaos in the CO oxidation reaction.

2. Experimental set-up and results

Experiments were performed in an ultrahigh-vacuum (UHV) chamber containing a Pt(110) single-crystal sample of 10 mm in diameter. For sample preparation, Ar-ion sputtering, oxygen treatment and annealing up to 900 K were used. Adsorbate concentration patterns on the sample surface were imaged using reflection–anisotropy microscopy (RAM; Rotermund *et al.* 1995). A schematic experimental set-up is shown in figure 1.

The reaction proceeds via a Langmuir–Hinshelwood mechanism where both oxygen and CO have to be adsorbed onto the catalytic surface before they can form CO_2 (Imbihl & Ertl 1995). In the experimental images shown here, dark areas reflect a reactive catalytic surface with high concentrations of O_{ad}, while on the brighter areas CO_{ad} dominates. Kinetic oscillations are induced by an adsorbate-driven phase transition of the platinum surface between the non-reconstructed 1×1 structure for CO-covered domains and a 1×2 missing row structure for oxygen-covered areas (Imbihl & Ertl 1995). This structural transition provides the optical contrast of our imaging method.

An Ar-ion laser was focused onto the crystal surface to a spot approximately 50 μm in diameter to induce localized temperature heterogeneity. The resulting temperature profile is of almost Gaussian shape with a maximum temperature increase of about 3 K for a laser power of 50 mW. Base temperature and partial pressures were chosen so that the reaction was in the oscillatory regime showing spatiotemporally chaotic dynamics.

In figure 2, the laser-induced initiation of a target pattern is shown. At $t=0$ s, the laser is moved to the position indicated by the white arrow in figure 2*a*, where after 20 s a growing target pattern can be observed that covers almost 50% of the

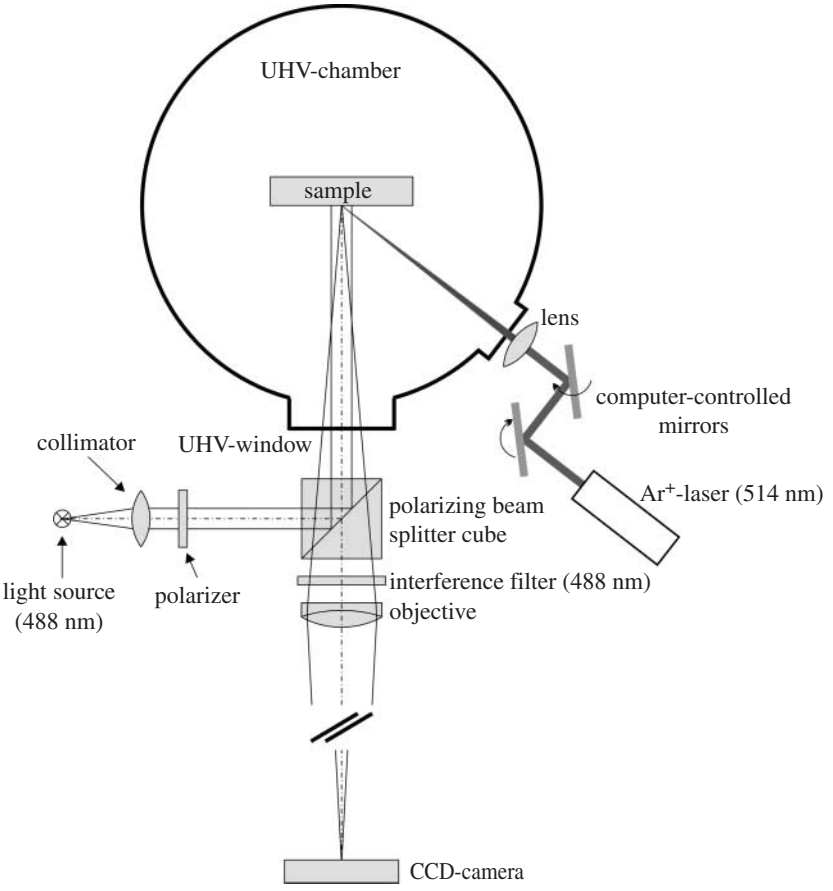

Figure 1. Schematic experimental set-up. Vertically pre-polarized light from the 488 nm line of an Ar-ion laser is reflected onto the Pt sample by a polarizing beam splitter cube. The polarization of the light reflected from the sample surface changes depending on surface reconstruction and adsorbate coverage. The component of the reflected light, which is now polarized in a parallel manner, is transmitted through the beam splitter and is used for the imaging of the crystal. Besides the imaging laser, an additional Ar-ion laser (514 nm) can be focused onto the Pt surface and its position can be adjusted via two computer-controlled galvanic mirrors. See also Qiao *et al.* (2006).

imaged surface area after 160 s (figure 2*b*,*c*). Eventually, turbulence was suppressed almost completely by the extending target pattern.

The local oscillation frequencies in the turbulent medium were measured and compared with the oscillation frequency at the location of the laser spot (figure 2*d*). To obtain the frequency spectra, image regions of 10×10 pixels were averaged at the indicated locations and their time-series were Fourier transformed. The frequency in the centre of the target pattern is increased by about 0.1 Hz with respect to the average frequency of the turbulent dynamics outside the target pattern. This is due to the temperature increase at the location of the laser spot (Wolff *et al.* 2004) and leads to the entrainment of the entire medium in the course of time.

If the laser spot was moved to another position on the surface, a new target pattern with the same frequency and wavelength appeared there after a latency period.

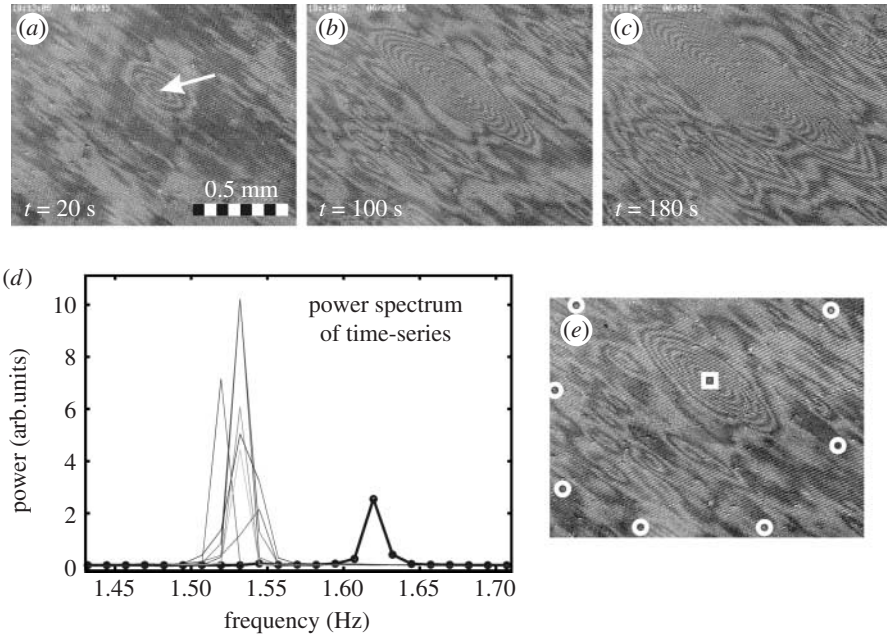

Figure 2. Growth of a target pattern created with focused laser light. (*a–c*) Time sequence snapshots and (*d*) local frequency spectra at the locations indicated with white circles in (*e*). The thick curve in (*d*) corresponds to the spectrum at the location of the laser spot (marked with an arrow in (*a*) and with a white square in (*e*)). Experimental parameters: $p_{CO}=7.84\times10^{-5}$ mbar, $p_{O_2}=1.84\times10^{-4}$ mbar, $T_0=538$ K, $P_{laser}=53$ mW.

3. Model and simulations

In this section, we present results from a numerical study of a realistic reaction model for the catalytic CO oxidation on Pt(110), the Krischer–Eiswirth–Ertl (KEE) model (Krischer *et al.* 1992). It consists of a system of three coupled partial differential equations,

$$\partial_t u = k_1 s_{CO} p_{CO}(1-u^3) - k_2 u - k_3 uv + D\nabla^2 u, \tag{3.1}$$

$$\partial_t v = k_4 p_{O_2}[s_{O,1\times1} w + s_{O,1\times2}(1-w)](1-u-v)^2 - k_3 uv \quad \text{and} \tag{3.2}$$

$$\partial_t w = k_5\left(\left[1+\exp\left(\frac{u_0-u}{\delta u}\right)\right]^{-1} - w\right), \tag{3.3}$$

where the variables u, v and w are normalized between 0 and 1 and represent the CO coverage, the oxygen coverage and the fraction of the surface found in the non-reconstructed 1×1 phase, respectively. Adsorption of CO and oxygen on the catalyst surface, desorption and surface diffusion of CO, as well as the reaction between the two adsorbed species are taken into account. Oxygen desorption and diffusion are negligible for the considered temperature ranges.

The temperature dependence of the rate constants of CO desorption, CO diffusion, surface reaction and surface structural phase transition is assumed to follow a simple Arrhenius-type relation, $k_i=\nu_i\exp(-E_i/k_B T)$. The impact of the laser on the reaction is modelled by a local increase in surface temperature and thus affects the

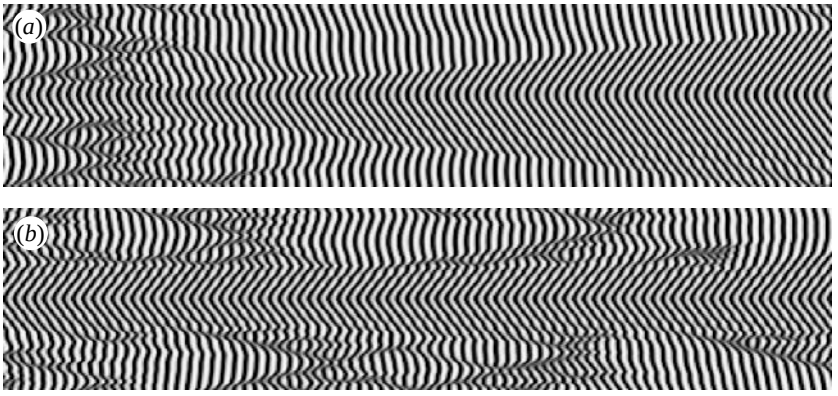

Figure 3. Chaos control induced by a local temperature shift. Target waves entrain completely (*a*) or partially (*b*) the turbulent state. (*a*) $\Delta T = 0.2$ K and $\sigma = 24$ μm; (*b*) $\Delta T = 0.225$ K and $\sigma = 12$ μm. Shown are space–time diagrams, where space runs along the vertical axis ($L = 800$ μm). The pacemaker was switched on for 100 s (*a*) and 200 s (*b*) before the displayed time interval $\Delta t = 200$ s. Shown is u (black corresponds to low CO coverage). Model parameters: $p_{\mathrm{CO}} = 4.46 \times 10^{-5}$ mbar, $p_{\mathrm{O}_2} = 1.1 \times 10^{-4}$ mbar, $T_0 = 543.47$ K, $k_1 = 3.14 \times 10^5$ s^{-1} mbar^{-1}, $k_2 = \nu_2 \exp(-E_2/k_{\mathrm{B}}T)$ with $\nu_2 = 2 \times 10^{16}$ s^{-1} and $E_2 = 38$ kcal mol^{-1}, $E_2 = 38$ kcal mol^{-1}, $k_3 = \nu_3 \exp(-E_3/k_{\mathrm{B}}T)$ with $\nu_3 = 3 \times 10^6$ s^{-1} and $E_3 = 10$ kcal mol^{-1}, $k_4 = 5.86 \times 10^5$ s^{-1} mbar^{-1}, $k_5 = \nu_5 \exp(-E_5/k_{\mathrm{B}}T)$ with $\nu_5 = 1056.1$ s^{-1} and $E_5 = 7$ kcal mol^{-1}, $s_{\mathrm{CO}} = 1.0$, $s_{\mathrm{O,1\times1}} = 0.6$, $s_{\mathrm{O,1\times2}} = 0.4$, $u_0 = 0.35$ and $\delta u = 0.05$, $D = D_0 \exp(-E_D/k_{\mathrm{B}}T)$ with $D_0 = 3.56 \times 10^6$ μm^2 s^{-1} and $E_D = 12.3$ kcal mol^{-1}.

dynamics by locally changing the abovementioned rate constants. Therefore, a stationary space-dependent temperature profile is introduced that shows a localized temperature rise at the location of the laser, $T = T_0 + \Delta T \exp[-(x - x_0)^2/(2\sigma^2)]$. The centre of the profile is chosen to coincide with the centre of the medium.

The KEE model was integrated numerically on a one-dimensional spatial domain using a forward Euler scheme and a nearest-neighbour representation of the Laplacian operator. Periodic boundary conditions were used. The system length is $L = 800$ μm, the grid length $\Delta x = 4$ μm and the time step $\Delta t = 0.001$ s.

The base temperature T_0 and the partial pressures p_{O_2} and p_{CO} are chosen such that a spatiotemporally chaotic state is observed. It is characterized by propagating defects that form and annihilate in cascades, and is commonly denoted as intermittent turbulence (Bertram & Mikhailov 2003). For the set of parameters considered here, intermittent turbulence coexists with uniform oscillations. However, for sufficiently large system sizes, most initial conditions lead to chaotic behaviour.

In figure 3*a*, we show a space–time diagram that demonstrates the transformation from the turbulent state to a target wave state due to a local temperature increase. Waves are created at the temperature heterogeneity and propagate outwards. Slowly, the waves suppress the turbulent regime, and the collision zone of the target waves with the turbulent wave fragments moves outwards. Finally, the entire medium is entrained by the pacemaker. In the state of control, the frequency of the target waves is larger than the average frequency of the turbulent pattern. This is typical for oscillatory media with positive dispersion where the pattern with the highest frequency eventually dominates over the other patterns.

In order to explore the domain of control, we show a numerically derived control diagram in figure 4*a*, where we keep the external parameters fixed and vary the temperature shift ΔT and the spot extension σ of the temperature heterogeneity. For

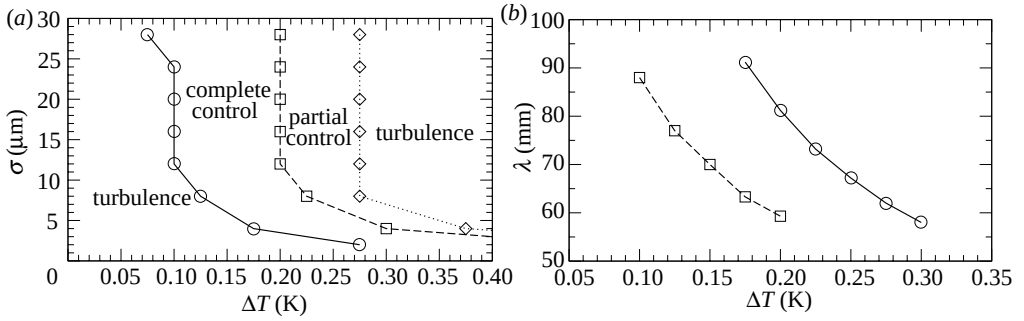

Figure 4. (*a*) Control diagram. Between and on the solid and dashed curves, stable target patterns are found. For a given spot extension, the temperature was increased in 0.025 K steps and simulations up to 1200 s were performed to check for asymptotic dynamics. (Usually, no qualitative changes were observed for simulation times longer than 400 s.) (*b*) Wavelengths of the stabilizing target waves for $\sigma = 4$ μm (solid line) and $\sigma = 24$ μm (dashed line). The wavelength decreases for increasing temperature. Parameters are the same as given in figure legend 3.

the values between the solid and the dashed curves (*complete control*), we observe the formation of an extending target pattern expelling the chaotic state as shown in figure 3*a*. To the left of the solid curve, the spot is too small for creating target waves that are able to suppress the turbulent dynamics. Between the dashed and the dotted curves (*partial control*), waves are emitted by the pacemaker but are unable to entrain the medium completely. Towards very small spot sizes, the temperature profile is not well resolved by the grid and the simulations are not conclusive.

Within the domains of control, the wavelength decreases with increasing temperature shift for a given spot extension. This is shown for two examples in figure 4*b*. Although for a small spot extension (solid line), larger temperatures are necessary to control spatiotemporal chaos than for a large spot extension (dashed line), the wavelengths of target waves that are able to suppress turbulence lie within the same range, approximately between 55 and 90 μm. This demonstrates that neither a specific temperature shift nor spot size is crucial to obtain control, as long as the wavelength of the resulting target waves lies in a particular efficient range. The upper boundary corresponds to the average distance between two wave fragments present in the turbulent regime. The lower boundary is related to the fact that a given oscillatory medium cannot support arbitrarily short wavelengths. For systems close to a supercritical Hopf bifurcation, the short-wavelength limit is determined by the so-called Eckhaus instability and has been thoroughly studied for heterogeneous pacemakers in the context of the complex Ginzburg–Landau equation (Stich & Mikhailov 2002, 2006).

As a consequence of this instability, waves with a wavelength shorter than a critical threshold become unstable and decay through phase slips in a finite distance from the wave source. As a result, a regime of short target waves is found close to the pacemaker, while in the far field turbulence prevails. Such a pattern is shown in figure 3*b*. In this case, the diameter of the target pattern is approximately 240 μm. Thus, there is a region of partial control, where the target pattern entrains its neighbourhood but is unable to control the entire medium. In this area, the extension of the target pattern decreases from left to right for a given spot extension.

An important difference between complete and partial control is that the behaviour of the system as the control force, that is the temperature

heterogeneity, is switched off. While the target waves slowly transform into stable uniform oscillations in the case of complete control, turbulence is recovered in the whole medium in the case of partial control.

4. Discussion

In this work, we suppress chemical turbulence in an experimentally accessible system, the catalytic CO oxidation on Pt(110). A localized perturbation was created by directing a focused laser beam onto the catalyst surface. At the location of the laser spot, the surface temperature was locally increased, leading to a rise in the frequency of kinetic oscillations about 0.1 Hz. This frequency shift was sufficient to create outward-travelling target waves that suppressed the initially turbulent state.

In earlier investigations (Stich *et al.* 2004; Wolff *et al.* 2004), it was found that three different wave patterns could be generated by laser-induced temperature heterogeneities. Depending on the choice of parameters, both outward- and inward-travelling target patterns could be created, as well as a spatially confined outward-travelling target pattern, related to the presence of global coupling through the gas phase.

While the previous experimental study has been performed in a regime where the unperturbed state of the system was characterized by uniform oscillations or regular wave patterns, in this study the initial state of the system consisted of chemical turbulence. Another difference is the imaging technique. Using RAM in the set-up shown above, we were able to observe the temporal dynamics of the reaction at the location of the laser spot.

Suppression of turbulence was also explored in the framework of the KEE model for the CO oxidation on Pt(110). Since we focused on turbulent states, gas-phase coupling could be neglected. In a series of simulations, the domain of control was determined in the plane spanned by the parameters ΔT and σ that characterize the magnitude and spatial extension of the localized perturbation. Here, two different regimes of control could be distinguished. The region of complete control is characterized by a target pattern that entrains the whole system, while for partial control—found for larger values of the frequency shift—only a finite area with constant radius around the pacemaker is filled by target waves. The main reason for control being lost is that high local frequencies are unable to create propagating stable target waves.

With respect to the parameters for studying the model, uniform oscillations and chemical turbulence were coexisting spatiotemporal solutions. If the laser was switched off after target waves had entrained the medium, the system relaxed to stable uniform oscillations in a phase diffusion scenario. If the pacemaker was switched off before complete control was reached, spatiotemporal chaos was recovered. This is in contrast to the situation reported in a recent numerical study of the complex Ginzburg–Landau equation (Jiang *et al.* 2004), in which uniform oscillations are unstable and turbulence is always recovered when control is switched off.

References

Battogtokh, D. & Mikhailov, A. 1996 Controlling turbulence in the complex Ginzburg–Landau equation. *Physica D* **90**, 84–95. (doi:10.1016/0167-2789(95)00232-4)

Bertram, M. & Mikhailov, A. S. 2003 Pattern formation on the edge of chaos: mathematical modeling of CO oxidation on a Pt(110) surface under global delayed feedback. *Phys. Rev. E* **67**, 036207. (doi:10.1103/PhysRevE.67.036207)

Bertram, M., Beta, C., Pollmann, M., Mikhailov, A. S., Rotermund, H. H. & Ertl, G. 2003*a* Pattern formation on the edge of chaos: experiments with CO oxidation on a Pt(110) surface under global delayed feedback. *Phys. Rev. E* **67**, 036208. (doi:10.1103/PhysRevE.67.036208)

Bertram, M., Beta, C., Rotermund, H. H. & Ertl, G. 2003*b* Complex patterns in a periodically forced surface reaction. *J. Phys. Chem. B* **107**, 9610–9615. (doi:10.1021/jp0341927)

Beta, C. & Mikhailov, A. S. 2004 Controlling spatiotemporal chaos in oscillatory reaction–diffusion systems by time-delay autosynchronization. *Physica D* **199**, 173–184. (doi:10.1016/j.physd.2004.08.012)

Beta, C., Bertram, M., Mikhailov, A. S., Rotermund, H. H. & Ertl, G. 2003 Controlling turbulence in a surface chemical reaction by time-delay autosynchronization. *Phys. Rev. E* **67**, 046224. (doi:10.1103/PhysRevE.67.046224)

Beta, C., Moula, M. G., Mikhailov, A. S., Rotermund, H. H. & Ertl, G. 2004 Excitable CO oxidation on Pt(110) under nonuniform coupling. *Phys. Rev. Lett.* **93**, 188302. (doi:10.1103/PhysRevLett.93.188302)

Imbihl, R. & Ertl, G. 1995 Oscillatory kinetics in heterogeneous catalysis. *Chem. Rev.* **95**, 697–733. (doi:10.1021/cr00035a012)

Jakubith, S., Rotermund, H. H., Engel, W., von Oertzen, A. & Ertl, G. 1990 Spatiotemporal concentration patterns in a surface reaction: propagating and standing waves, rotating spirals, and turbulence. *Phys. Rev. Lett.* **65**, 3013–3016. (doi:10.1103/PhysRevLett.65.3013)

Jiang, M., Wang, X., Ouyang, Q. & Zhang, H. 2004 Spatiotemporal chaos control with a target wave in the complex Ginzburg–Landau equation system. *Phys. Rev. E* **69**, 056202. (doi:10.1103/PhysRevE.69.056202)

Kim, M., Bertram, M., Pollmann, M., von Oertzen, A., Mikhailov, A. S., Rotermund, H. H. & Ertl, G. 2001 Controlling chemical turbulence by global delayed feedback: pattern formation in catalytic CO oxidation reaction on Pt(110). *Science* **292**, 1357–1360. (doi:10.1126/science.1059478)

Krischer, K., Eiswirth, M. & Ertl, G. 1992 Oscillatory CO oxidation on Pt(110): modelling of temporal self-organization. *J. Chem. Phys.* **96**, 9161–9172. (doi:10.1063/1.462226)

Ott, E., Grebogi, C. & Yorke, J. A. 1990 Controlling chaos. *Phys. Rev. Lett.* **64**, 1196–1199. (doi:10.1103/PhysRevLett.64.1196)

Qiao, L., Kevrekidis, I. G., Punckt, Ch. & Rotermund, H. H. 2006 Guiding chemical pulses through geometry: Y junctions. *Phys. Rev. E* **73**, 036219. (doi:10.1103/PhysRevE.73.036219)

Rotermund, H. H., Haas, G., Franz, R. U., Tromp, R. M. & Ertl, G. 1995 Imaging pattern formation in surface reactions from ultrahigh vacuum up to atmospheric pressures. *Science* **270**, 608–610. (doi:10.1126/science.270.5236.608)

Stich, M. & Mikhailov, A. S. 2002 Complex pacemakers and wave sinks in heterogeneous oscillatory systems. *Z. Phys. Chem.* **216**, 521–533.

Stich, M. & Mikhailov, A. S. 2006 Target patterns in two-dimensional heterogeneous oscillatory reaction–diffusion systems. *Physica D* **215**, 38–45. (doi:10.1016/j.physd.2006.01.011)

Stich, M., Ipsen, M. & Mikhailov, A. S. 2001 Self-organized stable pacemakers near the onset of birhythmicity. *Phys. Rev. Lett.* **86**, 4406–4409. (doi:10.1103/PhysRevLett.86.4406)

Stich, M., Beta, C., Wolff, J., & Rotermund, H. H. 2004 Inward traveling target patterns in the oscillatory CO oxidation on Pt(110). In *Experimental chaos: 8th Experimental Chaos Conf.* (eds S. Boccaletti, B. J. Gluckman, J. Kurths, L. M. Pecora, R. Meucci, & O. Yordanov), pp. 9–14. AIP Conf. Proc. no. 752, Melville, NY: AIP.

Wolff, J., Papathanasiou, A. G., Kevrekidis, I. G., Rotermund, H. H. & Ertl, G. 2001 Spatiotemporal addressing of surface activity. *Science* **294**, 134–137. (doi:10.1126/science.1063597)

Wolff, J., Stich, M., Beta, C. & Rotermund, H. H. 2004 Laser-induced target patterns in the oscillatory CO oxidation on Pt(110). *J. Phys. Chem. B* **108**, 14 282–14 291. (doi:10.1021/jp0498015)